

Varying-coefficient stochastic differential equations with applications in ecology

Théo Michelot*, Richard Glennie, Catriona Harris, Len Thomas

University of St Andrews, UK

Abstract

Stochastic differential equations (SDEs) are popular tools to analyse time series data in many areas, such as mathematical finance, physics, and biology. They provide a mechanistic description of the phenomenon of interest, and their parameters often have a clear interpretation. These advantages come at the cost of requiring a relatively simple model specification. We propose a flexible model for SDEs with time-varying dynamics where the parameters of the process are non-parametric functions of covariates, similar to generalized additive models. Combining the SDE and non-parametric approaches allows for the SDE to capture more detailed, non-stationary, features of the data-generating process. We present a computationally efficient method of approximate inference, where the SDE parameters can vary according to fixed covariate effects, random effects, or basis-penalty smoothing splines. We demonstrate the versatility and utility of this approach with three applications in ecology, where there is often a modelling trade-off between interpretability and flexibility.

*Email: tm75@st-andrews.ac.uk

1 Introduction

Stochastic differential equations (SDEs) describe the evolution of a system that involves stochastic noise (Allen, 2007). We present a general approach to improving the flexibility of such models. To introduce it, we focus on the most popular form of SDE,

$$dZ_t = \mu(Z_t, t) dt + \sigma(Z_t, t) dW_t, \quad Z_0 = z_0, \quad (1)$$

where (W_t) is a Wiener process, and z_0 is a known initial condition. The terms of the equation describe the evolution of the process (Z_t) : the drift μ measures the expected change in the process over an infinitesimal time interval, and the diffusion σ captures variability. In most applications, the drift and diffusion are chosen as simple parametric functions; the objective is to estimate their parameters and obtain a mechanistic description of the system. SDEs have, e.g., been applied in finance to study asset pricing (Aït-Sahalia and Kimmel, 2007), in biology to describe population dynamics (Dennis et al., 1991), and in epidemiology to predict disease spread (Allen and Van den Driessche, 2006). Eq. 1 includes Brownian motion, geometric Brownian motion, and the Ornstein-Uhlenbeck process as special cases.

SDEs are used to formulate a (simplified) description of a stochastic system, and the challenge is to build models flexible enough to reflect features of the system within the assumed structure of Eq. 1. For this purpose, there has been interest in specifying SDEs with time-varying dynamics. Regime-switching models have been developed, where a process switches between a finite number of SDEs, often based on an underlying continuous-time Markov chain (Mao and Yuan, 2006). These models combine the convenience of simple parametric models with the flexibility provided by multiple regimes, and have been used to describe, e.g., the movement of animals switching between behavioural states (Blackwell, 1997) or the time-varying dynamics of oil prices (Liechty and Roberts, 2001). An alternative is to specify the parameters of a SDE as continuous-valued random processes (e.g. Duan et al., 2009); e.g., in stochastic volatility models, the variance parameter of the diffusion function is itself specified as a diffusion process to account for changes in the variability (Aït-Sahalia and Kimmel, 2007). Other approaches have been developed to model the drift and diffusion of SDEs as non-parametric functions of time or of the value of the process Z_t , e.g. using Gaussian processes (Archambeau et al., 2007) or orthogonal Legendre polynomials (Rajabzadeh et al., 2016). For a particular class of SDEs applied to animal movement studies, Preisler et al. (2004) and Russell et al. (2018) suggested using splines to model the dependence of SDE parameters on spatial covariates.

We propose a general approach where the parameters of a SDE are specified as basis-

penalty smoothing splines, similar to generalized additive models (GAMs; Wood, 2017). This allows for a rich class of models including linear covariate effects, factor variables, independent random effects, and smooth (non-parametric) covariate effects. It stands in contrast to the regime-switching models where parameters are piecewise constant rather than smooth. It generalises the models where parameters are specified as Gaussian processes, given the equivalent interpretation of Gaussian processes and smoothing splines (Wood, 2017, Section 5.8.2), and it also extends ideas from Preisler et al. (2004) and Russell et al. (2018) to allow for flexible covariate dependence in a more general class of SDEs. We develop a method of inference, using a smoothing penalty in the SDE likelihood to control the roughness of non-parametric terms. We present a computationally efficient implementation based on the R packages `mgcv` and `TMB`, for model specification and model fitting, respectively.

We illustrate the potential of this new framework using three case studies from ecology. SDEs have great theoretical and practical appeal for the analysis of ecological data, because their continuous-time formulation does not depend on the sampling resolution of the data. Inferences from these models can therefore be compared across studies with different sampling schemes, and they can be fitted to data collected at irregular time intervals (e.g. Michelot and Blackwell, 2019). Despite their advantages, continuous-time models have been underutilised in this field, in part because they have lacked flexibility to specify time-varying dynamics and covariate effects, or have required computationally-costly model fitting procedures. The three case studies illustrate the utility of the new model over existing parametric approaches and highlight its flexibility and computational convenience. In the supplementary materials, we give implementation details, a simulation study, another case study from finance, and the source code to reproduce all analyses presented in the paper. The method that we describe is implemented in an R package, available at github.com/TheoMichelot/smoothSDE.

2 Varying-coefficient stochastic differential equations

2.1 Model formulation

We consider a stochastic process (Z_t) defined by

$$dZ_t = \mu(Z_t, \boldsymbol{\theta}_t) dt + \sigma(Z_t, \boldsymbol{\theta}_t) dW_t, \quad (2)$$

where the drift μ and diffusion σ depend on a time-varying parameter vector $\boldsymbol{\theta}_t$. We assume that μ and σ are known functions of Z_t and $\boldsymbol{\theta}_t$; they determine the type of stochastic process (e.g., Brownian motion, Ornstein-Uhlenbeck process). The parameter $\boldsymbol{\theta}_t$ depends on

time through its relationship with J temporal covariates $x_{1t}, x_{2t}, \dots, x_{Jt}$, and we write each component θ_t of $\boldsymbol{\theta}_t$ as

$$h(\theta_t) = \beta_0 + f_1(x_{1t}) + f_2(x_{2t}) + \dots + f_J(x_{Jt}),$$

where h is a link function, β_0 is an intercept parameter and, for $j = 1, \dots, J$, f_j could be a linear effect of a covariate, an independent random effect, or a smooth function. A simple example would be to have $x_{1t} = t$, to express that the dynamics of the process depend on time. For smooth functions or random effects, we employ the basis-penalty approach (Wood, 2017), writing the functions as linear combinations of m_j basis functions $\{\psi_{jk}\}$,

$$f_j(x) = \sum_{k=1}^{m_j} \beta_{jk} \psi_{jk}(x), \quad (3)$$

where several standard bases could be considered, e.g., cubic splines, thin plate regression splines, or B-splines. We will refer to this model as a varying-coefficient stochastic differential equation, as an analogy with the varying-coefficient models of Hastie and Tibshirani (1993).

2.2 Model fitting

We consider n observations (z_1, z_2, \dots, z_n) from the process (Z_t) , collected at (possibly irregular) times $t_1 < t_2 < \dots < t_n$. The aim is to estimate the relationship between the parameters $\boldsymbol{\theta}_t$ governing the drift and diffusion of the process and the covariates. The method that we propose is based on (1) the likelihood of the observations under the SDE model, and (2) a penalty added to the likelihood to control the roughness of non-parametric terms in $\boldsymbol{\theta}_t$.

2.2.1 Likelihood

Diffusion processes are Markovian, so the likelihood of n observations can be obtained as the product of the likelihoods of the individual transitions,

$$\begin{aligned} L(\boldsymbol{\alpha}, \boldsymbol{\beta} | z_1, \dots, z_n) &= [Z_{t_1} = z_1, \dots, Z_{t_n} = z_n] \\ &= [Z_{t_1} = z_1] \prod_{i=1}^{n-1} [Z_{t_{i+1}} = z_{i+1} | Z_{t_i} = z_i], \end{aligned} \quad (4)$$

where $\boldsymbol{\beta}$ contains the basis coefficients from Eq. 3 and $\boldsymbol{\alpha}$ is the vector of other parameters of the model (e.g., linear covariate effects), and where $[\cdot]$ is the pdf. The dependence on $\boldsymbol{\alpha}$ and $\boldsymbol{\beta}$ is omitted in the right-hand side of Eq. 4 for notational simplicity. We assume that the first value z_1 is deterministic, such that $[Z_{t_1} = z_1] = 1$.

Evaluating the likelihood requires computation of the transition density $[Z_{t_{i+1}}|Z_{t_i}]$ of the process. For many common processes, such as Brownian motion, geometric Brownian motion, and the Ornstein-Uhlenbeck process, this density has an analytical expression. In such cases, the transition density of the corresponding varying-coefficient process can be approximated by assuming that the parameter $\boldsymbol{\theta}_t$ is fixed over each time interval of observation. Then, the time-varying parameter $\boldsymbol{\theta}_{t_i}$ can be substituted into the transition density of the standard process. However, many SDEs of the form given in Eq. 2 do not have a closed-form transition density. More generally, we can then use the Euler-Maruyama discretization, and approximate the transition density $[Z_{t_{i+1}}|Z_{t_i} = z_i]$ by the pdf of a normal distribution with mean $z_i + \mu(z_i, \boldsymbol{\theta}_{t_i})\Delta_i$ and variance $\sigma(z_i, \boldsymbol{\theta}_{t_i})^2\Delta_i$, where $\Delta_i = t_{i+1} - t_i$. This approximation assumes that the drift and diffusion terms are constant over each interval $[t_i, t_{i+1})$ between two observations. We present the varying-coefficient versions of several common processes in Appendix A, and give their approximate transition densities. Substituting the approximate transition density into Eq. 4 yields the approximate likelihood for the full data set.

This method of inference is not exact, because it uses the transition density of the time-discretized diffusion process. The Euler-Maruyama discretization has the advantage of being widely applicable and easy to implement, but the accuracy of the estimation will decrease for longer time intervals between observations. To mitigate the effects of this approximation, we could include additional time points in the time series of observed data, corresponding to “missing” observations, and integrate over them, e.g., using either Markov chain Monte Carlo methods or the Laplace approximation (Elerian et al., 2001; Albertsen, 2019). Adding these missing values to the grid of observations leads to a finer time resolution, and improves the accuracy of the approximation, such that the error can be made arbitrarily small.

The process (Z_t) might sometimes not be observed directly, in which case the problem of inference is slightly different. This can be viewed as a state-space model, where the state equation is given by the transition density $[Z_{t_{i+1}}|Z_{t_i}]$ (e.g., obtained using the Euler approximation), and the observation equation is the density $[\tilde{Z}_{t_i}|Z_{t_i}]$, where \tilde{Z}_{t_i} denotes the observations. In this context, \tilde{Z}_t could e.g. include measurement error or be a more general function of Z_t . The diffusion process of interest is a latent process in the model, and it must be marginalised over to obtain the likelihood of the observed data. In the case of a Gaussian linear state-space model, the Kalman filter can be implemented, with time-varying parameters, and the likelihood obtained as a by-product. In this case, the Kalman filter can also be used to integrate over missing data in a data augmentation scheme to improve the discretization approximation. One example of a latent-state SDE is the velocity

Ornstein-Uhlenbeck model described by Johnson et al. (2008), where the observed process (location) is the integral of a diffusion process (velocity). In that model, the location process is smooth, and it is therefore convenient to describe the persistent movement of an animal or particle, or other processes with strong autocorrelation. Non-Gaussian state-space models can also be accommodated using Markov chain Monte Carlo or the Laplace approximation to marginalise over the state process, as suggested, e.g., by Albertsen et al. (2015). We present two examples of state-space SDE models in Section 3.

2.2.2 Smoothing penalty

Within the basis-penalty approach of GAMs, the roughness of the smoothing splines can be penalised in the likelihood, to obtain smooth relationships between the parameter θ_t and the covariates. The penalised log-likelihood is

$$l_p(\boldsymbol{\alpha}, \boldsymbol{\beta}, \boldsymbol{\lambda} | z_1, \dots, z_n) = \log\{L(\boldsymbol{\alpha}, \boldsymbol{\beta} | z_1, \dots, z_n)\} - \sum_j \lambda_j \boldsymbol{\beta}_j^T \mathbf{S}_j \boldsymbol{\beta}_j, \quad (5)$$

where $L(\boldsymbol{\alpha}, \boldsymbol{\beta} | z_1, \dots, z_n)$ is the unpenalised likelihood given in Eq. 4, $\boldsymbol{\beta}_j$ is the vector of basis coefficients, \mathbf{S}_j is the smoothing matrix associated with the chosen penalty, and λ_j is a smoothness parameter for the j -th smooth term in θ_t (Wahba, 1990). \mathbf{S}_j is a matrix of known coefficients, and it is constructed such that $\boldsymbol{\beta}_j^T \mathbf{S}_j \boldsymbol{\beta}_j$ measures the roughness (wiggleness) of the corresponding smooth term (Wood, 2017). The penalised log-likelihood can then be used to perform maximum likelihood estimation, or Bayesian inference can be performed if the penalty is viewed as an improper prior on the basis coefficients.

In Eq. 5, the penalised log-likelihood is expressed in terms of the degrees of smoothness $\boldsymbol{\lambda} = (\lambda_1, \lambda_2, \dots)$ of the smoothing splines. In most applications, $\boldsymbol{\lambda}$ is unknown, and it must be estimated from the data. Here, we consider the marginal likelihood approach, i.e., we treat the basis coefficients $\boldsymbol{\beta}$ of the splines as random effects, and integrate them out of the likelihood. This yields the marginal likelihood of the smoothness parameters $\boldsymbol{\lambda}$ and other fixed parameters $\boldsymbol{\alpha}$,

$$L(\boldsymbol{\alpha}, \boldsymbol{\lambda} | z_1, \dots, z_n) = \int L(\boldsymbol{\alpha}, \boldsymbol{\beta} | z_1, \dots, z_n) [\boldsymbol{\beta} | \boldsymbol{\lambda}] d\boldsymbol{\beta}, \quad (6)$$

where $[\boldsymbol{\beta} | \boldsymbol{\lambda}]$ is the density of a multivariate normal distribution with mean zero and block-diagonal precision matrix. Each block of the precision matrix corresponds to the penalty for the basis coefficients of one smoothing spline, and it can be written $\lambda_j \mathbf{S}_j$. As with standard GAMs, various basis-penalty smooths could be used. In the applications of Section 3, we considered thin plate regression splines, which are optimal in the sense defined by Wood

(2003), with a shrinkage penalty to ensure that the smooth terms shrink to zero when the penalty tends to infinity (Marra and Wood, 2011).

2.2.3 Implementation

The marginal likelihood can be implemented in the R package TMB, which uses the Laplace approximation to integrate over the random effects (Kristensen et al., 2016), and the design matrices for the basis functions and the penalty matrices can be computed with the R package mgcv (Wood, 2017). A numerical optimiser (e.g., `optim` or `nlminb`) can then be used to minimise the marginal likelihood, and obtain estimates of the smoothness parameter λ and fixed effects α . We can get predicted values for the random effects β , analogous to best linear unbiased predictors in linear mixed effect models, to infer the smooth relationships between SDE parameters and covariates. The joint precision matrix of fixed and random effects can be used for uncertainty quantification.

TMB makes it relatively simple to include other random effects in the model. It is often the case, e.g. in animal movement or financial studies, that the data arise from multiple instances of the SDE (multiple animals, stocks, etc.) and one wishes to fit a model that combines these instances while also allowing for inter-individual variation. The case of i.i.d. normal random effects is easily handled, as it is another type of basis-penalty smoother, where the penalty matrix is the identity matrix (Wood, 2017, Section 7.7).

We describe the details of the implementation of this method, using mgcv and TMB, in Appendix B. We ran simulation experiments to investigate the performance of the proposed approach to recover the relationship between the SDE parameters and the covariates, under several model formulations. In those simulations, we thinned the simulated data to irregular time intervals, to mimic a real data set, and the method performed well in all scenarios (Appendix C). We also performed a simulation experiment to check the coverage of confidence intervals derived for θ_t using the precision matrix given by TMB, and found that they correctly represented the uncertainty in the estimates (Appendix C).

2.3 Model selection and model checking

In this framework, it might be useful to discriminate between competing model formulations, e.g., different forms of the drift and diffusion terms. The problem of model selection in models involving basis-penalty smooths is relatively understudied outside standard GAMs. Wood (2017) describes two versions of the Akaike Information Criterion (AIC), the *marginal* AIC and the *conditional* AIC, based on different forms of the likelihood and AIC penalty (i.e.,

number of parameters in basic AIC). The marginal AIC uses the marginal likelihood defined in Eq. 6 with a penalty for the number of fixed effects α and smoothing parameters λ , and would be straightforward to implement in the framework of Section 2.2.3. The conditional AIC is based on the joint penalised likelihood of fixed and random effects (Eq. 5), with an additional AIC penalty on the complexity of smooth terms (given by the number of effective degrees of freedom; see Section 5.4.2 of Wood, 2017). For more detail about the respective limitations of these two criteria and possible solutions, see Section 6.11 of Wood (2017). An alternative approach for model selection is to include an additional penalty in the likelihood, so that model components can be shrunk to zero (i.e., removed from the model) as part of the smoothness parameter estimation (Marra and Wood, 2011).

For a chosen formulation, we propose a simple diagnostic to investigate goodness-of-fit in varying-coefficient SDE models. Based on the Euler-Maruyama discretisation of the process, a natural choice for model residuals ϵ_i is

$$\epsilon_i = \frac{z_{i+1} - (z_i + \mu(z_i, \hat{\theta}_{t_i})\Delta_i)}{\sigma(z_i, \hat{\theta}_{t_i})\sqrt{\Delta_i}},$$

for $i = 1, \dots, n - 1$, using the notation of Section 2.2.1, and where $\hat{\theta}_{t_i}$ is the estimate of θ_t over $[t_i, t_{i+1})$. Under the assumptions of the model (and of the discretisation), the residuals should be independent and approximately follow a standard normal distribution. In the analysis of Section 3.3, we use quantile-quantile plots of the residuals to investigate lack of fit, and autocorrelation function plots to identify residual autocorrelation.

3 Illustrative examples

In this section, we present three analyses based on ecological data, to illustrate different applications of the models presented in Section 2. We stress, however, that the varying-coefficient approach is general to SDE modelling, and our focus is chosen only because we are most familiar with these ecological problems. To further demonstrate the generality of the method, we also provide the analysis of a financial data set of oil prices in Appendix D.

3.1 Linking elephant movement to environmental conditions

We illustrate the utility of varying-coefficient SDEs to analyse animal movement data, using the trajectory of an African elephant (*Loxodonta africana*) presented by Wall et al. (2014b) and available on the Movebank data repository (Wall et al., 2014a). We restricted the analysis to a period from May to September 2009 to avoid seasonal effects. The data set consisted

of a time series of 3652 Easting-Northing locations, and also included the air temperature measured by the tag, at a time resolution of 1 hour (with a few missing observations).

We used a varying-coefficient version of the continuous-time correlated random walk model presented by Johnson et al. (2008); the original model has been used extensively to analyse animal location data. In this model, the (unobserved) velocity \mathbf{V}_t of the animal is formulated as a varying-coefficient Ornstein-Uhlenbeck process,

$$d\mathbf{V}_t = -r_t \mathbf{V}_t dt + s_t d\mathbf{W}_t,$$

where r_t and s_t can be linked to the speed and sinuosity of the movement. This is a special case of the varying-coefficient SDE of Eq. 2 where $\mu(\mathbf{V}_t, t) = -r_t \mathbf{V}_t$ and $\sigma(\mathbf{V}_t, t) = s_t$, i.e., with parameters $\boldsymbol{\theta}_t = (r_t, s_t)$. (Although the process \mathbf{V}_t is bivariate, it is isotropic and the two dimensions can therefore be treated as two univariate processes driven by the same parameters.) Because the velocity is unobserved, the model can be written as a state-space model where \mathbf{V}_t is latent, and where the observed process is the location of the animal, obtained as $\mathbf{Z}_t = \mathbf{Z}_0 + \int_0^t \mathbf{V}_s ds$. As described in Section 2.2.1, we implemented the likelihood using a Kalman filter with time-varying parameters. To investigate the effects of environmental conditions on the elephant's behaviour, we estimated the parameters r_t and s_t of the velocity process as functions of the air temperature. For interpretation, we then derived the parameter $\nu_t = \sqrt{\pi} s_t / (2\sqrt{r_t})$, described by Gurarie et al. (2017) as a measure of the speed of movement of the animal. Model fitting took about 5 min on a 1.3GHz Intel i7 CPU.

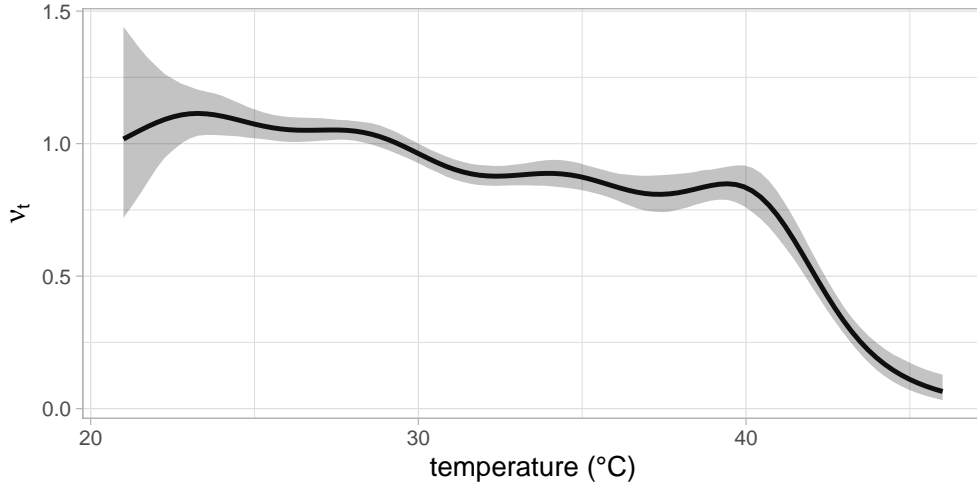


Figure 1: Results of the elephant analysis. Estimates of the speed parameter $\nu_t = \sqrt{\pi} s_t / (2\sqrt{r_t})$, as a function of temperature. The black line is the mean estimate, and the grey shaded area is a 95% confidence band.

Figure 1 shows estimates of the speed parameter ν_t as a function of temperature. A small value of ν_t corresponds to slow movement, encompassing behaviours with little activity (e.g., resting), and a large value corresponds to more active behaviours (e.g., exploration, transit). The speed parameter was highest at low temperatures (20-30 degrees), and decreased for higher temperatures, with a very steep decline above 40 degrees. This is consistent with what is known of the species: elephants are very sensitive to heat, and spend much of their time resting or waiting in the shade during periods of high temperatures (Mole et al., 2016). Our non-parametric approach illuminated the non-linear relationship between the temperature and the speed of movement of this elephant.

Other varying-coefficient models have been proposed in movement ecology to capture the effects of time-varying covariates on animal behaviour. In particular, Hanks et al. (2015) modelled animal movement over a discrete spatial grid as a continuous-time Markov chain with time-varying transition rates, and linked transition rates to covariates using basis functions (similarly to Eq. 3). This continuous-time discrete-space model and its extensions have, e.g., been used to investigate the effects of time-varying environmental conditions on the movements of cougars (Hanks et al., 2015; Buderman et al., 2018), fur seals, and ants (Hanks and Hughes, 2016). The varying-coefficient SDEs presented in this paper offer an alternative framework to incorporate similar covariate effects in the dynamics of continuous-valued random processes (e.g., the continuous location or velocity of an animal).

SDEs have also been popular for analysing animal tracking data, e.g., to model animal behaviour (Blackwell, 1997), the effects of environmental features on movement decisions (Preisler et al., 2004; Michelot et al., 2019), and the emergence of home ranges (Dunn and Gipson, 1977). Regime-switching SDEs have been developed to allow for time-varying dynamics in the movement, where the latent state represents the behaviour of the animal (Blackwell, 1997; Michelot and Blackwell, 2019). However, discrete behavioural states may lack the flexibility to capture the wide range of behaviours that animals display. It has also been difficult to include general covariate effects in that context; inference has typically required computationally-costly custom algorithms (Blackwell et al., 2016). The method we propose to include factor covariates, linear or smooth effects of continuous covariates, and random effects in SDE models is an important step forward to link animal movement behaviour to environmental and individual-specific conditions.

The output of regime-switching models (classification of data into clusters) may sometimes be more readily interpretable than the smoothly-varying parameters suggested here. In such cases, we could use a clustering algorithm on the estimated θ_t values to identify different

regimes in the time series, and interpret each cluster based on its centre, say. This procedure could be repeated on posterior draws of θ_t to account for uncertainty in the clustering.

Preisler et al. (2004) and Russell et al. (2018) presented application-specific methods to define smooth relationships between movement parameters and spatial covariates in SDEs. The approach presented in this paper is a generalisation of their work to a wider class of SDEs, where any parameters can be specified using basis-penalty smooths. Note that the varying-coefficient CTCRW model could be fitted with the R package *crawl* (Johnson et al., 2008; Johnson and London, 2018), using the joint likelihood of all parameters rather than the marginal likelihood of Eq. 6. That package does not implement the smoothness parameter estimation and this would need to be done in an additional model selection stage.

3.2 Body condition of elephant seals

We considered a study of body condition of elephant seals described by Schick et al. (2013), where the authors modelled body fat content over time, and how it was affected by environmental conditions. We used the data set from Pirotta et al. (2019), which includes information about drift dives of 26 Northern elephant seals (*Mirounga angustirostris*). The goal of the study was to investigate the dynamics of the body fat content of seals during migratory foraging trips, which last several months. Animals’ body fat content cannot be observed directly when they are at sea. However, using telemetry tags fitted with depth sensors, we can measure the rate at which seals drift vertically in the water column during non-active dives (“drift dives”; Biuw et al., 2003). This drift rate is linked to the percentage of body fat because fat content affects buoyancy. A natural modelling approach, proposed by Schick et al. (2013), is therefore to treat body fat content as a latent process in a state-space model, and estimate how it changes during a foraging trip from the drift rate observations.

We formulated a continuous-time analogue of the model of Schick et al. (2013), and defined the body fat content L_t as a Brownian motion with time-varying drift, i.e., $dL_t = r_t dt + \sigma dW_t$ (Eq. 2 with $\mu(L_t, t) = r_t$ and $\sigma(L_t, t) = \sigma$). The time-varying parameter r_t measured the daily rate of change of the lipid content, with larger values indicating faster accumulation of fat mass. We combined the above SDE with the observation equation proposed by Schick et al. (2013) to obtain the following state-space model formulation

$$\begin{aligned} \text{Observation process} \quad D_i &\sim N\left(\alpha_1 + \alpha_2 \frac{L_i}{R_i}, \frac{\tau^2}{h_i}\right) \\ \text{State process} \quad L_{i+1} &\sim N(L_i + r_i \Delta_i, \sigma^2 \Delta_i) \end{aligned}$$

where i is the day index, D_i is the mean drift rate, L_i is the lipid content, R_i is the non-lipid content, h_i is the number of drift dives, and α_1 , α_2 and τ are parameters of the observation process. We followed Schick et al. (2013) in assuming a constant diffusion σ , and investigated the effects of two covariates on the lipid change rate r_t : (1) surface transit per day, and (2) distance to the colony where the animals were tagged. We chose these covariates to link fat gains (i.e., foraging behaviour) to movement patterns and geographical location. In preliminary analyses, we included two other covariates from Schick et al. (2013) (body fat proportion at departure, and daily number of drift dives), but found no evidence of an effect. We included a random normal intercept in r_t to account for differences between seals.

We implemented the likelihood of this model with the Kalman filter, and estimated the effects of the covariates on the drift parameter following Section 2. Schick et al. (2013) fitted their state-space model within a Bayesian framework, using informative priors for τ^2 and σ^2 based on biological knowledge. We included the same prior distributions as multiplicative terms in the likelihood, therefore performing maximum posterior estimation for those parameters. Model fitting took about 2 min on a 1.3GHz Intel i7 CPU.

Results are shown in Figure 2. The lipid gain rate r_t was estimated to decrease with daily transit distance, which is consistent with the findings of Schick et al. (2013). This suggests that lipid gains are low when seals are travelling at high speeds, and that foraging is characterized by less horizontal movement. We also found that lipid gains increased with distance to the colony, in particular between 0 and 2000km. This indicates that animals must travel a considerable distance from their breeding colony to find foraging grounds that are rich enough for them to start gaining fat. Figure 2 shows a map of the movement tracks of the seals, coloured by the predicted value of r_t , which highlights portions of the trips with high lipid gains. Our results provide a mechanistic justification for the assumption often made in elephant seal studies that slow horizontal movement at sea is associated with foraging behaviour (e.g., Michelot et al., 2017).

This application shows how SDEs can be built as alternatives to discrete-time models (such as the state-space model of Schick et al., 2013), which do not depend on the time resolution of the data and can be applied to data collected at irregular intervals. Another difference with Schick et al. (2013) is that we implemented the Kalman algorithm and Laplace approximation (with TMB) to integrate over latent components of the model, whereas they used computationally-costly Markov chain Monte Carlo methods.

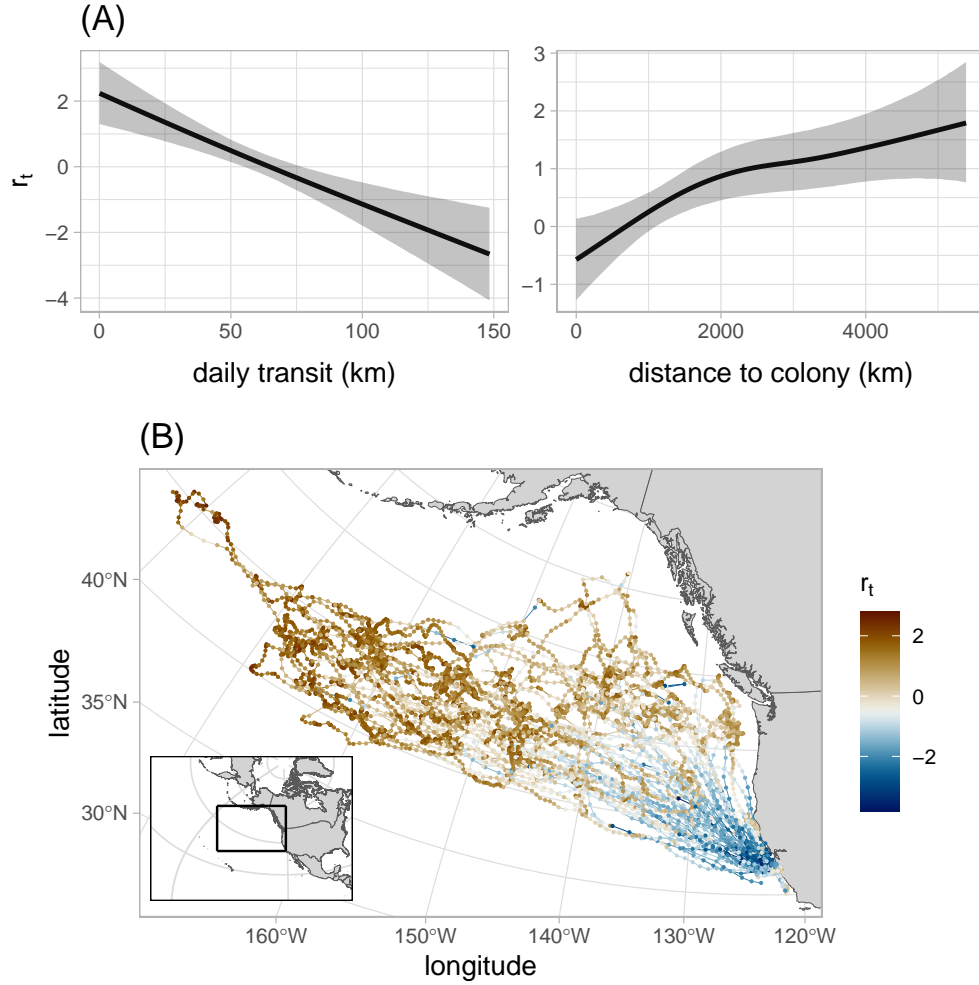


Figure 2: Results of elephant seal body condition study. (A) Estimated relationship between lipid gain parameter r_t and two covariates: daily transit distance (left), and distance to colony (right). The black lines are mean estimates, and the grey shaded areas are 95% confidence bands. Each estimate was obtained by fixing the other covariate to its mean. (B) Elephant seal movement tracks, coloured by predicted value of r_t . This figure appears in color in the electronic version of this article.

3.3 Diving behaviour of beaked whales

Beaked whales are marine mammals that routinely dive to depths in excess of 1km for periods of over an hour. Animal-borne telemetry tags allow study of their diving behaviour (Johnson and Tyack, 2003; DeRuiter et al., 2013). Here we consider data collected from high-resolution tags that include accelerometer and magnetometer sensors (“DTAGs”; Johnson and Tyack, 2003), attached to four Cuvier’s beaked whales (*Ziphius cavirostris*). In general, beaked whales display two different types of dives with different physiological functions: deep and shallow dives. The structures of deep and shallow dives are very distinct, and would require separate models. Here, we focused on shallow dives, and also excluded sections of the data where the animals were at the sea surface (depth < 15 m). The data set comprised $n_d = 73$ shallow dives from the four whales, with a median duration of 23 min. Multiple variables can be derived from DTAG data, and we computed the Euler angles (pitch, roll, and heading), which describe the posture of the animal in the water (Johnson and Tyack, 2003). The pitch is the angle between the main body axis and the horizontal, the roll is the angle around the main body axis, and the bearing is the angle in the horizontal plane (Figure S4 of supplementary material). The sampling rate of the raw data varied between 5Hz and 25Hz, and we downsampled by taking averages over non-overlapping 5-sec windows, to reduce the computational cost while keeping a sufficiently fine resolution to detect behavioural changes over each dive. This resulted in a total of 20041 observations for each variable.

Visual inspection of the data suggested that shallow dives all had a similar structure, with different phases of each dive displaying different levels of activity. Our aim was therefore to characterise the typical behaviour of beaked whales, as measured by their postural dynamics, during the different diving phases (e.g., descent, ascent, bottom). In preliminary analyses, we tried modelling each variable (pitch, roll, heading) with Brownian motion, but residual analysis revealed that the model did not capture heavy tails in increments of the process. We therefore replaced the Gaussian transition density with a generalized t distribution with fixed degrees of freedom ($\nu = 3$, based on visual data exploration), and estimated the location parameter r_t and the scale parameter s_t as time-varying. Here, we used the Euler-Maruyama discretization of the process (rather than the SDE itself) as the “model of record” to build a more complex model, as suggested by Brillinger (2010) in a similar context. Although this model is not a special case of the SDE given in Eq. 2, the method described in Section 2 can be applied, with the likelihood defined the pdf of a t distribution for each observed transition. The details of the model are described in Appendix E of the supplementary material. For this example, the three processes were treated as independent.

The model had two parameters: the location r_t and scale s_t of the t-distributed increments. To investigate the time-varying behaviour of beaked whales, we specified r_t and s_t as smooth functions of the proportion of time through the dive $x_t \in [0, 1]$. We treated the dives as independent, and included random intercepts for the dive in r_t and s_t , to account for variability between individuals and between dives. In summary, there were six time-varying parameters (r_t and s_t for each of the three data variables), modelled for each variable as

$$\begin{aligned} r_t &= \zeta_{d_t} + f_r(x_t), & \zeta_j &\sim N(\mu_\zeta, (\sigma_\zeta)^2) \text{ for } j \in \{1, 2, \dots, n_d\}, \\ \log(s_t) &= \xi_{d_t} + f_s(x_t), & \xi_j &\sim N(\mu_\xi, (\sigma_\xi)^2) \text{ for } j \in \{1, 2, \dots, n_d\}, \end{aligned}$$

where $d_t \in \{1, 2, \dots, n_d\}$ is the dive index at time t , f_r and f_s are basis-penalty smooths, and $\{\mu_\zeta, \sigma_\zeta, \mu_\xi, \sigma_\xi\}$ are unknown hyper-parameters. Model fitting took 30 min on a 1.3GHz Intel i7 CPU. The estimated relationships between the parameters and the proportion of time through the dive are shown in Figure 3.

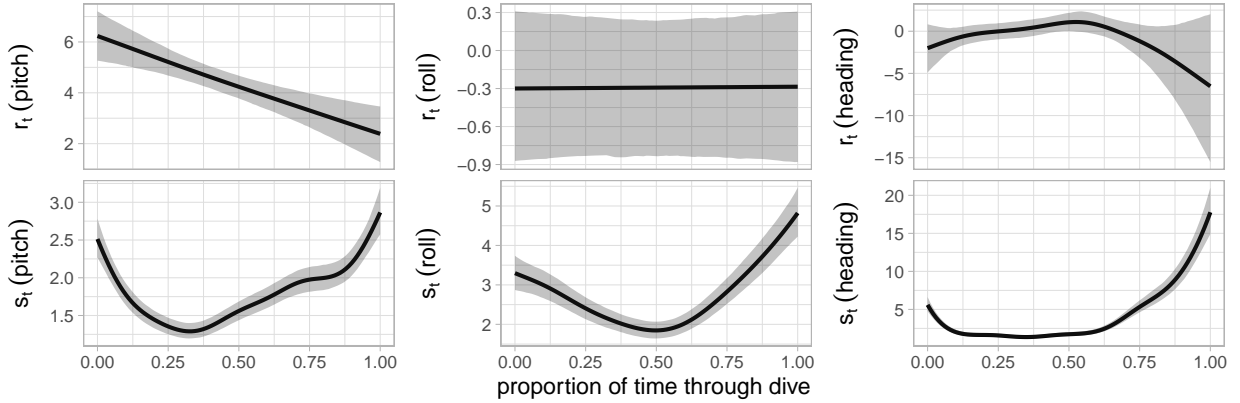


Figure 3: Estimates of the drift (r_t , top row) and diffusion (s_t , bottom row) parameters as functions of the proportion of time through the dive, in the beaked whale analysis. The three columns correspond to the three modelled variables: pitch (left), roll (middle), and heading (right). The black lines are the mean estimates, and the grey shaded areas are 95% confidence bands. All estimates were obtained with the mean random effect intercept.

The estimated drift parameter r_t for pitch was positive over the whole dive, suggesting that pitch tended to increase during a typical dive. This is consistent with the observed convex shape of the dives: pitch increases between the descent and bottom phases, and again between the bottom and ascent phases. The estimated drift for roll was close to zero, and did not seem to be affected by the phase of the dive, suggesting that there were no particular trend in that variable. The estimated drift in heading was negative during the final part of the dive (ascent), but the confidence bands were wide and overlapped zero. All

three diffusion parameters s_t suggested that there was more variability at the start and end of each dive, i.e. during ascent and descent, than when the whale was at the bottom. This variability can be viewed as a proxy for the level of activity: more diffusion suggests more frequent postural changes. Variability in pitch was low during the bottom phase, which may be associated with gliding motion, whereas it was high during descent and ascent, suggesting continued stroking or “stroke-and-glide” motion. These changes in the pitch diffusion parameter showed how whales alternate between different swimming styles over each dive, which has been linked to energetic efficiency in response to drag forces and buoyancy (Miller et al., 2004; Martín López et al., 2015). Roll displayed highest variability during the ascent phase, and the diffusion parameter for heading was much higher during the final phase of the dive, just before the whales surfaced again, corresponding to more directional changes in the horizontal plane. These postural changes may have several functions, such as locating predators before surfacing (when the whales are most vulnerable), socialising with conspecifics, and orienting to sea currents.

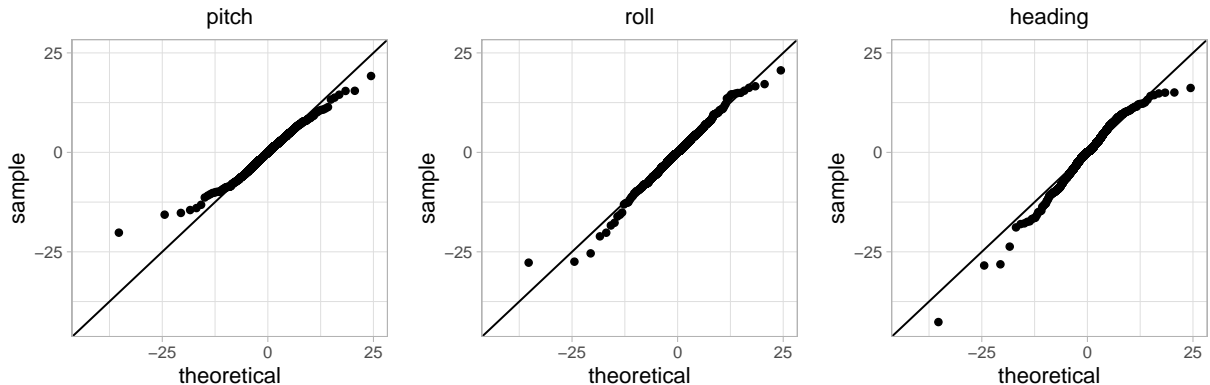


Figure 4: Quantile-quantile plots of the residuals against the Student’s t distribution with $\nu = 3$ degrees of freedom, for the beaked whale analysis.

Quantile-quantile plots of the residuals against the appropriate standardized t distributions are shown in Figure 4, and suggest appropriate fit. However, we found autocorrelation in the residuals using autocorrelation function plots, pointing to features of the whales’ movement that were not included in the model (Figure S5 of the supplementary material). Most notably, there was positive autocorrelation in the heading residuals over about 1-2 minutes, suggesting that some persistence in heading was not captured by the model. It might be more adequate to model heading with a process that induces correlation between increments, such as a one-dimensional version of the continuous-time correlated random walk used in Section 3.1. There was no correlation between residuals of the three processes (pitch, roll,

and heading), supporting our decision to model them separately.

Most existing analyses of DTAG data have been based on dive-by-dive summary statistics of activity (e.g., dive duration, maximum depth), and have looked at broad behavioural patterns (e.g., DeRuiter et al., 2013; Quick et al., 2017). This contrasts with our approach, where the behaviour of beaked whales is modelled at a fine time resolution over each dive, and the dives are treated as realisations of an underlying random process. Using varying-coefficient SDEs, we could estimate a more detailed description of the within-dive activity of whales. As another alternative, discrete-time regime-switching models have been proposed to analyse data of this kind (i.e., hidden Markov models; Isojunno and Miller, 2015; Leos-Barajas et al., 2017), and a similar continuous-time approach could be implemented. In that setting, the states of the latent process would represent discrete regimes of activity. For high-resolution data, however, it may often be preferable to model behaviour as changing smoothly in time (rather than switching between discrete states). The method that we use also makes it straightforward to investigate the effects of covariates (if available), and to include random effects to capture differences between individuals.

4 Discussion

In this paper, we have focused on a univariate diffusion process (Z_t) , and suggested using independent diffusion processes for each dimension in the case of multivariate data (e.g., the three postural angles in Section 3.3). The proposed method could similarly be applied to the N -dimensional diffusion process (\mathbf{Z}_t) defined by the equation $d\mathbf{Z}_t = \boldsymbol{\mu}(\mathbf{Z}_t, \boldsymbol{\theta}_t)dt + \boldsymbol{\sigma}(\mathbf{Z}_t, \boldsymbol{\theta}_t)d\mathbf{W}_t$, where $\boldsymbol{\mu}(\mathbf{Z}_t, \boldsymbol{\theta}_t) \in \mathbb{R}^N$, $\mathbf{W}_t \in \mathbb{R}^N$, and $\boldsymbol{\sigma}(\mathbf{Z}_t, \boldsymbol{\theta}_t) \in \mathbb{R}^{N \times N}$. In this case, the drift $\boldsymbol{\mu}$ and diffusion $\boldsymbol{\sigma}$ might be functions of several time-varying parameters. We can use the Euler-Maruyama discretization to obtain the (approximate) transition density as a multivariate normal distribution, and estimate the model parameters as in Section 2. A simulation study may be required to investigate identifiability in such models, when a large number of time-varying parameters must be estimated jointly.

The method of inference that we presented in Section 2 is approximate, as it relies on the time discretization of the drift and diffusion functions. As suggested in Section 2.2.1, data augmentation can be used to improve the accuracy of the method, but there are no general guidelines as to when this might be necessary. Recent studies have evaluated the approximation error of the Euler-Maruyama method for special cases of SDEs (Albertsen, 2019; Michelot et al., 2019), but the performance of the approach will be application-specific.

The discretization is based on the assumption that the SDE parameters θ_t are fixed over each time interval, i.e., the error depends on how fast θ_t varies over time. Future work could focus on developing diagnostics to assess the time resolution of discretization, e.g. based on the distribution of first-order differences in estimated values of θ_t .

The parameters of a varying-coefficient SDE are specified using basis-penalty smooths, and we therefore assume a smooth relationship between parameters and covariates. There is some flexibility in this formulation, because the smoothness parameter is estimated from the data, but it may not always be appropriate. In particular, if the relationship involves abrupt changes (e.g., discontinuities), then it may not be well captured by a smooth function, and regime-switching models may be preferable. To better understand this issue, it would be interesting to compare the results of the varying-coefficient approach and a regime-switching model on the same data set. However, this may not be straightforward in practice, as there is no generally-applicable method to include covariates in continuous-time regime-switching models. We could also consider integrating regime switches into varying-coefficient SDEs, i.e., defining each SDE parameter by several smooths between which the process switches through time. This model can be viewed as a continuous-time hidden Markov model where the state-dependent observation distribution is given by the transition density of the SDE, and the approximate likelihood of this model could be obtained using existing methodology.

We suggested using the package TMB to implement the marginal likelihood and to integrate over random effects using the Laplace approximation. TMB also uses automatic differentiation to evaluate the gradient of the log-likelihood, which improves computational speed (Kristensen et al., 2016). This fast implementation has a downside: to build the gradient function, TMB needs to create the “computational graph” of the likelihood, i.e., its representation in terms of elementary functions (for which the analytical gradient is known). In our experience, the construction of this graph can be memory-intensive for large data sets or complex model formulations, and may not be feasible on standard desktop computers. In those cases, high-performance computing systems with more memory may be required.

The model presented for the time-varying parameters of SDEs relies on the general methodology of generalized additive models (GAMs), which has been greatly extended beyond the basic formulation presented herein. In particular, an interesting direction for future research will be the implementation of hierarchical GAMs (Pedersen et al., 2019) in this framework. Here, the smooth relationship between response and covariates can vary across groups, while retaining some common features (related to shape and degree of smoothness). This extension could be applied to investigate inter-individual differences in ecological anal-

yses, with more nuance than the simple random-intercept model mentioned in Section 2.2.3. We could, e.g., define the response of several animals to an environmental covariate with functions comprising a population-level mean component and individual-level components measuring the individual deviations from the mean. Other extensions of GAMs, such as adaptive smoothing (Wood, 2017, Section 5.3.5) or tensor product smooth interactions (Wood, 2017, Section 5.6), could further increase the applicability of varying-coefficient SDEs.

Acknowledgments

We would like to thank Simon Chamaillé-Jammes, Stacy DeRuiter, Alan Gelfand, Josh Hewitt, Dave Miller, Nicola Quick, and Rob Schick for fruitful discussions about this research, as well as the reviewers and editors for suggestions that greatly improved the paper. This work was funded by the US Office of Naval Research, grant N000141812807. The beaked whale data of Section 3.3 was collected as part of the SOCAL-BRS project, primarily funded by the US Navy’s Chief of Naval Operations Environmental Readiness Division and subsequently by the US Navy’s Living Marine Resources Program. Additional support for environmental sampling and logistics was also provided by the Office of Naval Research, Marine Mammal Program. All research activities for that study were authorized and conducted under US National Marine Fisheries Service permit 14534; Channel Islands National Marine Sanctuary permit 2010-004; US Department of Defense Bureau of Medicine and Surgery authorization; a federal consistency determination by the California Coastal Commission; and numerous institutional animal care and use committee authorizations. We are grateful to Jake Wall, George Wittemyer, Valerie LeMay, Iain Douglas-Hamilton and Brian Klinkenberg for making the elephant data used in Section 3.1 publicly available, and to Enrico Pirotta, Lisa Schwarz, Daniel Costa, Patrick Robinson and Leslie New for making the elephant seal data used in Section 3.2 publicly available.

References

- Aït-Sahalia, Y. and Kimmel, R. (2007). Maximum likelihood estimation of stochastic volatility models. *Journal of Financial Economics*, 83(2):413–452.
- Albertsen, C. M. (2019). Generalizing the first-difference correlated random walk for marine animal movement data. *Scientific Reports*, 9(1):1–14.
- Albertsen, C. M., Whoriskey, K., Yurkowski, D., Nielsen, A., and Flemming, J. M. (2015). Fast fitting of non-Gaussian state-space models to animal movement data via Template Model Builder. *Ecology*, 96(10):2598–2604.

- Allen, E. (2007). *Modeling with Itô stochastic differential equations*, volume 22. Springer Science & Business Media.
- Allen, L. J. and Van den Driessche, P. (2006). Stochastic epidemic models with a backward bifurcation. *Mathematical Biosciences & Engineering*, 3(3):445.
- Archambeau, C., Cornford, D., Opper, M., and Shawe-Taylor, J. (2007). Gaussian process approximations of stochastic differential equations. *Journal of Machine Learning Research*, 1:1–16.
- Biuw, M., McConnell, B., Bradshaw, C. J., Burton, H., and Fedak, M. (2003). Blubber and buoyancy: monitoring the body condition of free-ranging seals using simple dive characteristics. *Journal of Experimental Biology*, 206(19):3405–3423.
- Blackwell, P. G. (1997). Random diffusion models for animal movement. *Ecological Modelling*, 100(1-3):87–102.
- Blackwell, P. G., Niu, M., Lambert, M. S., and LaPoint, S. D. (2016). Exact Bayesian inference for animal movement in continuous time. *Methods in Ecology and Evolution*, 7(2):184–195.
- Brillinger, D. R. (2010). Modeling spatial trajectories. In Gelfand, A., Diggle, P., Guttorp, P., and Fuentes, M., editors, *Handbook of Spatial Statistics*, pages 463–474. CRC Press, Boca Raton, Florida, USA.
- Buderman, F. E., Hooten, M. B., Alldredge, M. W., Hanks, E. M., and Ivan, J. S. (2018). Time-varying predatory behavior is primary predictor of fine-scale movement of wildland-urban cougars. *Movement Ecology*, 6(1):22.
- Dennis, B., Munholland, P. L., and Scott, J. M. (1991). Estimation of growth and extinction parameters for endangered species. *Ecological Monographs*, 61(2):115–143.
- DeRuiter, S. L., Southall, B. L., Calambokidis, J., Zimmer, W. M., Sadykova, D., Falcone, E. A., Friedlaender, A. S., Joseph, J. E., Moretti, D., Schorr, G. S., et al. (2013). First direct measurements of behavioural responses by Cuvier’s beaked whales to mid-frequency active sonar. *Biology Letters*, 9(4):20130223.
- Duan, J. A., Gelfand, A. E., Sirmans, C., et al. (2009). Modeling space-time data using stochastic differential equations. *Bayesian Analysis*, 4(4):733–758.

- Dunn, J. E. and Gipson, P. S. (1977). Analysis of radio telemetry data in studies of home range. *Biometrics*, 33(1):85–101.
- Elerian, O., Chib, S., and Shephard, N. (2001). Likelihood inference for discretely observed nonlinear diffusions. *Econometrica*, 69(4):959–993.
- García, C. A., Otero, A., Felix, P., Presedo, J., and Marquez, D. G. (2017). Nonparametric estimation of stochastic differential equations with sparse Gaussian processes. *Physical Review E*, 96(2):022104.
- Gurarie, E., Fleming, C. H., Fagan, W. F., Laidre, K. L., Hernández-Pliego, J., and Ovaskainen, O. (2017). Correlated velocity models as a fundamental unit of animal movement: synthesis and applications. *Movement Ecology*, 5(1):13.
- Hanks, E. M., Hooten, M. B., Alldredge, M. W., et al. (2015). Continuous-time discrete-space models for animal movement. *The Annals of Applied Statistics*, 9(1):145–165.
- Hanks, E. M. and Hughes, D. A. (2016). Flexible discrete space models of animal movement. *arXiv preprint arXiv:1606.07986*.
- Hastie, T. and Tibshirani, R. (1993). Varying-coefficient models. *Journal of the Royal Statistical Society: Series B (Methodological)*, 55(4):757–779.
- Isojunno, S. and Miller, P. J. (2015). Sperm whale response to tag boat presence: biologically informed hidden state models quantify lost feeding opportunities. *Ecosphere*, 6(1):1–46.
- Johnson, D. S. and London, J. M. (2018). crawl: an R package for fitting continuous-time correlated random walk models to animal movement data.
- Johnson, D. S., London, J. M., Lea, M.-A., and Durban, J. W. (2008). Continuous-time correlated random walk model for animal telemetry data. *Ecology*, 89(5):1208–1215.
- Johnson, M. P. and Tyack, P. L. (2003). A digital acoustic recording tag for measuring the response of wild marine mammals to sound. *IEEE Journal of Oceanic Engineering*, 28(1):3–12.
- Kristensen, K., Nielsen, A., Berg, C., Skaug, H., and Bell, B. (2016). TMB: Automatic differentiation and Laplace approximation. *Journal of Statistical Software*, 70(5):1–21.

- Leos-Barajas, V., Photopoulou, T., Langrock, R., Patterson, T. A., Watanabe, Y. Y., Murgatroyd, M., and Papastamatiou, Y. P. (2017). Analysis of animal accelerometer data using hidden Markov models. *Methods in Ecology and Evolution*, 8(2):161–173.
- Liechty, J. C. and Roberts, G. O. (2001). Markov chain Monte Carlo methods for switching diffusion models. *Biometrika*, 88(2):299–315.
- Mao, X. and Yuan, C. (2006). *Stochastic differential equations with Markovian switching*. Imperial College Press.
- Marra, G. and Wood, S. N. (2011). Practical variable selection for generalized additive models. *Computational Statistics & Data Analysis*, 55(7):2372–2387.
- Martín López, L. M., Miller, P. J., Aguilar de Soto, N., and Johnson, M. (2015). Gait switches in deep-diving beaked whales: biomechanical strategies for long-duration dives. *Journal of Experimental Biology*, 218(9):1325–1338.
- Michélot, T. and Blackwell, P. G. (2019). State-switching continuous-time correlated random walks. *Methods in Ecology and Evolution*, 10(5):637–649.
- Michélot, T., Gloaguen, P., Blackwell, P. G., and Étienne, M.-P. (2019). The Langevin diffusion as a continuous-time model of animal movement and habitat selection. *Methods in Ecology and Evolution*, 10(11):1894–1907.
- Michélot, T., Langrock, R., Bestley, S., Jonsen, I. D., Photopoulou, T., and Patterson, T. A. (2017). Estimation and simulation of foraging trips in land-based marine predators. *Ecology*, 98(7):1932–1944.
- Miller, P. J., Johnson, M. P., Tyack, P. L., and Terray, E. A. (2004). Swimming gaits, passive drag and buoyancy of diving sperm whales *Physeter macrocephalus*. *Journal of Experimental Biology*, 207(11):1953–1967.
- Mole, M. A., Rodrigues D’Áraujo, S., Van Aarde, R. J., Mitchell, D., and Fuller, A. (2016). Coping with heat: behavioural and physiological responses of savanna elephants in their natural habitat. *Conservation Physiology*, 4(1).
- Pedersen, E. J., Miller, D. L., Simpson, G. L., and Ross, N. (2019). Hierarchical generalized additive models in ecology: an introduction with mgcv. *PeerJ*, 7:e6876.

- Pirotta, E., Schwarz, L. K., Costa, D. P., Robinson, P. W., and New, L. (2019). Modeling the functional link between movement, feeding activity, and condition in a marine predator. *Behavioral Ecology*, 30(2):434–445.
- Preisler, H. K., Ager, A. A., Johnson, B. K., and Kie, J. G. (2004). Modeling animal movements using stochastic differential equations. *Environmetrics*, 15(7):643–657.
- Quick, N. J., Isojunno, S., Sadykova, D., Bowers, M., Nowacek, D. P., and Read, A. J. (2017). Hidden Markov models reveal complexity in the diving behaviour of short-finned pilot whales. *Scientific Reports*, 7(1):1–12.
- Rajabzadeh, Y., Rezaie, A. H., and Amindavar, H. (2016). A robust nonparametric framework for reconstruction of stochastic differential equation models. *Physica A: Statistical Mechanics and its Applications*, 450:294–304.
- Russell, J. C., Hanks, E. M., Haran, M., Hughes, D., et al. (2018). A spatially varying stochastic differential equation model for animal movement. *The Annals of Applied Statistics*, 12(2):1312–1331.
- Schick, R. S., New, L. F., Thomas, L., Costa, D. P., Hindell, M. A., McMahon, C. R., Robinson, P. W., Simmons, S. E., Thums, M., Harwood, J., et al. (2013). Estimating resource acquisition and at-sea body condition of a marine predator. *Journal of Animal Ecology*, 82(6):1300–1315.
- Uhlenbeck, G. E. and Ornstein, L. S. (1930). On the theory of the Brownian motion. *Physical Review*, 36(5):823.
- Vasicek, O. (1977). An equilibrium characterization of the term structure. *Journal of Financial Economics*, 5(2):177–188.
- Wahba, G. (1990). *Spline models for observational data*. SIAM, Philadelphia.
- Wall, J., Wittemyer, G., LeMay, V., Douglas-Hamilton, I., and Klinkenberg, B. (2014a). Data from: Elliptical time-density model to estimate wildlife utilization distributions. Movebank data repository, DOI:10.5441/001/1.f321pf80/1.
- Wall, J., Wittemyer, G., LeMay, V., Douglas-Hamilton, I., and Klinkenberg, B. (2014b). Elliptical time-density model to estimate wildlife utilization distributions. *Methods in Ecology and Evolution*, 5(8):780–790.

- Wood, S. N. (2003). Thin plate regression splines. *Journal of the Royal Statistical Society: Series B (Statistical Methodology)*, 65(1):95–114.
- Wood, S. N. (2017). *Generalized additive models: an introduction with R*. CRC press. Second Edition.

Appendix A Special cases with applications in ecology and finance

The specification of the functions μ and σ in the SDE determines the type of diffusion process (Equation 2 of the paper). In practice, this choice depends on the characteristics of the observed process. In this section, we propose several choices of μ and σ , corresponding to varying-coefficient variants of standard diffusion processes, and possible applications to the analysis of animal movement and other ecological data. In all the examples that we consider here, the drift function μ and the diffusion function σ each depend on only one time-varying parameter, i.e. $\mu(Z_t, \boldsymbol{\theta}_t) = \mu(Z_t, \theta_t^{(1)})$ and $\sigma(Z_t, \boldsymbol{\theta}_t) = \sigma(Z_t, \theta_t^{(2)})$, where $\boldsymbol{\theta}_t = (\theta_t^{(1)}, \theta_t^{(2)})$. We denote $r_t = \theta_t^{(1)}$ and $s_t = \theta_t^{(2)}$ for simplicity.

Brownian motion with drift The simplest model is the Brownian motion (with drift), where $\mu(Z_t, \boldsymbol{\theta}_t) = r_t$ and $\sigma(Z_t, \boldsymbol{\theta}_t) = s_t$. Here, r_t and s_t are time-varying drift and diffusion parameters for the process, respectively. Based on the Euler-Maruyama discretization, the approximate transition density of this process is

$$[Z_{t+\Delta} = z_{t+\Delta} | Z_t = z_t] = \phi(z_{t+\Delta}; z_t + r_t \Delta, s_t^2 \Delta),$$

where $\phi(x; m, v)$ is the pdf of the normal distribution with mean m and variance v .

Geometric Brownian motion The process Z_t is called geometric Brownian motion if $\log(Z_t)$ follows a Brownian motion with drift. The varying-coefficient geometric Brownian motion is a diffusion process with $\mu(Z_t, \boldsymbol{\theta}_t) = r_t Z_t$ and $\sigma(Z_t, \boldsymbol{\theta}_t) = s_t Z_t$. Geometric Brownian motion is a popular choice to model population growth in ecology, where Z_t is the population size at time t , and r_t is the growth rate (Dennis et al., 1991), which could be modelled as a function of covariates in the framework that we present.

This process is also used in finance to describe asset prices under the Black-Scholes model. In addition, stochastic volatility models are typically based on geometric Brownian motion, where the variance parameter s_t^2 is modelled with an SDE (Aït-Sahalia and Kimmel, 2007). The varying-coefficient model introduced here is an alternative approach to specify a process with time-varying volatility.

The standard geometric Brownian motion has a closed form transition density, and so we can obtain the transition density of the varying-coefficient process by substituting r_t and

s_t for the SDE parameters,

$$[Z_{t+\Delta} = z_{t+\Delta} | Z_t = z_t] = \frac{1}{\sqrt{2\pi\Delta}} \frac{1}{z_{t+\Delta}s_t} \exp \left[-\frac{\{\log(z_{t+\Delta}) - \log(z_t) - (r_t - 0.5s_t^2)\Delta\}^2}{2s_t^2\Delta} \right].$$

Ornstein-Uhlenbeck (OU) The varying-coefficient OU process is obtained with $\mu(Z_t, \theta_t) = r_t(\zeta - Z_t)$ and $\sigma(Z_t, \theta_t) = s_t$. It is mean-reverting, i.e. it tends to revert to its mean value ζ with a rate measured by r_t and diffusion measured by s_t . The standard OU process was proposed by Uhlenbeck and Ornstein (1930) to describe the velocity of a particle subject to friction, and it has also been proposed as a model for interest rates in finance (Vasicek, 1977). Figure S1 shows a realisation from the varying-coefficient OU process, to illustrate how time-varying parameters can induce time-varying dynamics. The approximate transition density of the varying-coefficient OU process is

$$[Z_{t+\Delta} = z_{t+\Delta} | Z_t = z_t] = \phi \left\{ z_{t+\Delta}; \zeta + e^{-r_t\Delta}(z_t - \zeta), \frac{s_t^2}{2r_t}(1 - e^{-2r_t\Delta}) \right\}.$$

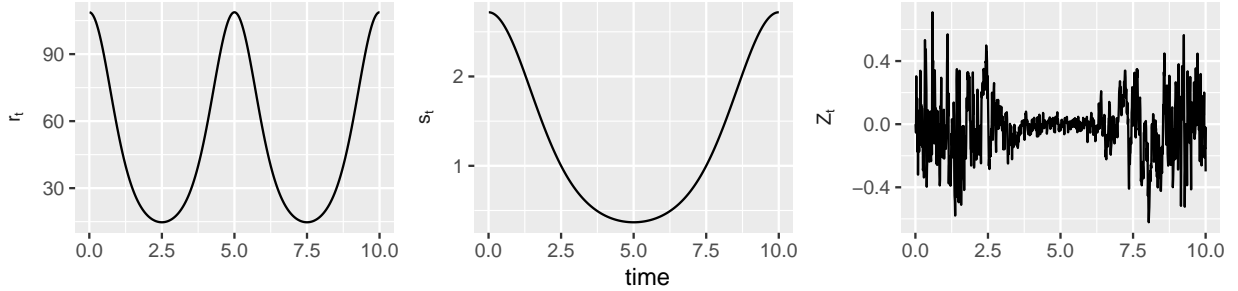


Figure S1: Simulated example for the time-varying Ornstein-Uhlenbeck process with mean $\zeta = 0$, showing the reversion parameter r_t (left), the diffusion parameter s_t (middle) and the simulated process Z_t (right).

Dunn and Gipson (1977) suggested the bivariate OU process as a model of movement for animals displaying home range behaviour: in two dimensions, mean reversion is analogous to attraction to a point in space, such as the centre of an animal's home range. The long-term distribution of the OU process is Gaussian, and can be derived in closed form. In that context, r_t and s_t can be linked to the size of the home range, and the strength of attraction to a central location. In practice, V_t and Z_t are usually two-dimensional (representing Easting and Northing), but it is most common to assume that the process is isotropic, i.e. the same process describes the movement in both dimensions. Blackwell (1997) argued that the OU process may often be too simplistic to model the movement of animals, and proposed a

mixture model, where an animal switches between discrete behaviours through time, each associated with an OU process. In the framework presented here, r_t and s_t are specified as flexible functions of covariates, as described in Section 2 of the manuscript, and the dynamics of the OU process can therefore change smoothly over time and space. The number of time-varying parameters in the model is not limited to two (r_t and s_t), and the centre of attraction ζ could in principle also be formulated as a function of covariates.

The OU process is also a popular model for the *velocity* of a moving animal, as proposed by Johnson et al. (2008). In the varying-coefficient variant of this model, the velocity V_t is specified as $dV_t = r_t(\zeta - V_t)dt + s_t dW_t$, and the location Z_t of the animal is obtained as the integral $Z_t = Z_0 + \int_0^t V_s ds$, where Z_0 is the initial location. Here, the two parameters r_t and s_t can be linked to the speed and persistence of the movement, and ζ is usually set to zero to indicate that there is no systematic bias in the velocity. Several approaches have been developed to allow for time-varying dynamics in the velocity OU model. In particular, Michelot and Blackwell (2019) presented a state-switching formulation, where an animal transitions between different velocity OU processes through time, characterised by different movement characteristics. Russell et al. (2018) used a time-varying term for the centre of attraction ζ , to include covariate effects on the direction of movement of the animal. The model presented here generalises that approach to the case where any parameter of the velocity process can be written as a GAM of spatiotemporal (or other) covariates.

Potential-based models In ecology, diffusion processes have also been used to study the response of animals to their environment. For this purpose, the drift of the process can be specified as a function of the gradient of a “potential” function H , which measures habitat suitability over space (Preisler et al., 2004). In that model, we have $\mu(Z_t, \boldsymbol{\theta}_t) = -\nabla H(Z_t, \boldsymbol{\theta}_t)$, where ∇ is the spatial gradient operator. Preisler et al. (2004) estimated H with smoothing splines of spatial covariates, using methodology similar to that presented in this paper. Within the framework that we propose, their model could be extended to include non-spatial covariates, and to investigate covariate effects on the diffusion parameter of the process (which they assumed constant).

Appendix B Implementation

B.1 Model matrices using mgcv

The mgcv R package can be used to define the design matrices (including basis functions) and the penalty matrix for basis-penalty smooths, with the function `gam` (Wood, 2017). As an example, consider the data frame shown below, where ‘ID’ is the time series identifier, ‘Z’ is the response variable, and ‘x1’ and ‘x2’ are two covariates.

```
##   ID      Z      x1      x2
## 1  1 -1.06520105 1.139137 -0.3088276
## 2  1 -1.36064381 2.159093 -0.1593682
## 3  1 -1.04660349 2.610276 -0.6394209
## 4  1  0.35250424 1.830601 -0.7986991
## 5  1 -0.07465397 1.905763  0.4524077
## 6  1 -0.91468379 2.124810  0.3858297
```

Then, consider that Z is to be modelled with a varying-coefficient SDE, where the relationship of each SDE parameter with the covariates is specified by the following formula,

```
# Formula for SDE parameter, using mgcv syntax for smooth
# terms and random effects
form <- ~ x1 + s(x2, k = 5, bs = "ts") + s(ID, bs = "re")
```

i.e. x1 has a linear effect, x2 has a smooth effect modelled using thin-plate regression splines, and a random normal intercept is included for ID. (See the documentation of mgcv for additional detail on the syntax.) The design matrices can then be derived as follows,

```
# Create smooth object using mgcv
smooth <- gam(formula = update(form, dummy ~ .),
              data = cbind(dummy = 1, data),
              fit = FALSE)

# Design matrix
X <- smooth$X
```

```

# Number of non-smooth model terms (i.e. fixed effects)
nsdf <- smooth$nsdf

# Design matrix for fixed effects
X_fe <- X[, 1:nsdf, drop = FALSE]

# Design matrix for random effects (including smooth model terms)
X_re <- X[, -(1:nsdf), drop = FALSE]

```

The design matrix for the fixed effects is

```

head(X_fe)

##      (Intercept)      x1
## 1             1 1.139137
## 2             1 2.159093
## 3             1 2.610276
## 4             1 1.830601
## 5             1 1.905763
## 6             1 2.124810

```

and the design matrix for the random effects is

```

head(X_re)

##                                     ID1 ID2 ID3 ID4
## 1 -0.2064242 0.6333093 0.4155266 -0.12492927  1  0  0  0
## 2 -0.1186081 0.6690554 0.4211488 -0.06103063  1  0  0  0
## 3 -0.3930194 0.5225471 0.3865907 -0.26626842  1  0  0  0
## 4 -0.4775210 0.4553437 0.3648461 -0.33436490  1  0  0  0
## 5  0.2464654 0.7122938 0.3947111  0.20052304  1  0  0  0
## 6  0.2071078 0.7157652 0.4013989  0.17205880  1  0  0  0

```

where the first four columns correspond to the four basis functions for x_2 , and the four last columns are dummy indicator variables for ID. Then, the linear predictor for the SDE parameter is

```
lp <- X_fe %*% coeff_fe + X_re %*% coeff_re
```

where `coeff_fe` and `coeff_re` are the coefficients for the fixed effects and the random effects, respectively. The SDE parameter (at each time point) is then obtained by applying the inverse link function to this linear predictor.

Similarly, the penalty matrix for the smooth terms can be extracted from the GAM object,

```
S <- smooth$S
```

B.2 Laplace approximation using TMB

The model fitting procedure proposed in the paper requires the evaluation of the marginal likelihood, where the random effects (including basis coefficients for smooth terms) have been integrated out. We suggest using the R package Template Model Builder (TMB) to implement the marginal likelihood, based on the Laplace approximation Kristensen et al. (2016). Here, we broadly explain how TMB can be used to evaluate the objective function (i.e., the negative log-likelihood) of the model, and to obtain point and uncertainty estimates for the model parameters.

The joint log-likelihood must first be written in C++, following the TMB syntax (for examples, see kaskr.github.io/adcomp/examples.html). For our model, it has two main components:

1. the joint log-likelihood of the fixed and random effect parameters, given by the sum of the log-pdf of the observed transitions, $\log[Z_{i+1}|Z_i]$, e.g. obtained using the Euler-Maruyama discretization of the process. This part requires the SDE parameters on a time grid, which can be computed based on the model matrices provided by `mgcv`, as described in Appendix B.1.
2. the log-pdf of the basis coefficients (and other random effects) given the smoothness parameter, $\log[\boldsymbol{\beta}|\boldsymbol{\lambda}]$, obtained as the log of a multivariate normal pdf with block-diagonal precision matrix, where the i -th block is $\lambda_i \mathbf{S}_i$. The smoothness matrix \mathbf{S}_i is provided by `mgcv`, as described in Appendix B.1.

The C++ function takes the following arguments as data:

- times of observations (t_1, \dots, t_n) ;

- observations (z_1, \dots, z_n)
- design matrix for fixed effects (`X_fe` in Appendix B.1), provided by `mgcv`;
- design matrix for random effects (`X_re` in Appendix B.1), provided by `mgcv`;
- smoothness matrix (`S` in Appendix B.1), provided by `mgcv`;

and the following arguments as parameters:

- coefficients for fixed effects (`coeff_fe` in Appendix B.1);
- coefficients for random effects (`coeff_re` in Appendix B.1);
- smoothness parameters λ .

The objective function (and its gradient) can then be defined in R with the TMB function `MakeADFun` applied to the joint negative log-likelihood, using the argument ‘random’ to specify that the basis coefficients `coeff_re` should be treated as random effects. It can then be passed to a numerical optimiser, e.g. `optim` or `nlm`, to perform maximum likelihood estimation of the fixed effect parameters. After optimisation, the function `sdreport` can be used to obtain estimates of the random effect parameters, as well as a joint precision matrix for the fixed and random effects. Posterior samples of all model parameters can be generated from a multivariate normal distribution, where the covariance matrix is the inverse of this precision matrix.

B.3 Package `smoothSDE`

This method is implemented in the R package `smoothSDE`, available at github.com/TheoMichelot/smoothSDE. The package provides functions for model fitting, uncertainty estimation, model checking, and model plots, and we hope that it will greatly facilitate the application of varying-coefficient SDEs. Here, we present the code required to fit the varying-coefficient model applied to the elephant data set from Wall et al. (2014b), in Section 3.2 of the main text, to showcase its use.

First, we download the data from the Movebank data repository, and create a data frame with columns for ID, time (as numeric), response variables (here, easting and northing), and covariates (here, temperature),

```

# Load package and set seed for reproducibility
library(smoothSDE)
set.seed(58652)

# Load data and keep relevant columns
URL <- paste0("https://www.datarepository.movebank.org/bitstream/handle/",
              "10255/move.373/Elliptical%20Time-Density%20Model%20%28Wall%",
              "20et%20al.%202014%29%20African%20Elephant%20Dataset%20%",
              "28Source-Save%20the%20Elephants%29.csv")
raw <- read.csv(url(URL))
keep_cols <- c(11, 13, 14, 17, 6)
raw_cols <- raw[, keep_cols]
colnames(raw_cols) <- c("ID", "x", "y", "date", "temp")

# Only keep five months to eliminate seasonal effects
track <- subset(raw_cols, ID == unique(ID)[1])
track$date <- as.POSIXlt(track$date, tz = "GMT")
track$time <- as.numeric(track$date - min(track$date))/3600
keep_rows <- which(track$date > as.POSIXct("2009-05-01 00:00:00") &
                  track$date < as.POSIXct("2009-09-30 23:59:59"))
track <- track[keep_rows,]

# Convert to km
track$x <- track$x/1000
track$y <- track$y/1000

```

```

# Data set including ID, time, responses (x, y), and covariate (temp)
head(track)

```

##	ID	x	y	date	temp	time
## 9689	Salif Keita	572.3427	1675.424	2009-05-01 00:00:00	33	9703
## 9690	Salif Keita	572.5443	1675.392	2009-05-01 01:00:00	32	9704
## 9691	Salif Keita	572.6159	1675.339	2009-05-01 02:00:00	31	9705
## 9692	Salif Keita	572.7745	1675.101	2009-05-01 03:00:00	31	9706


```
## 9693 Salif Keita 572.8844 1675.065 2009-05-01 04:00:00 31 9707
## 9694 Salif Keita 573.6659 1674.322 2009-05-01 05:00:00 30 9708
```

For this analysis, we use the velocity Ornstein-Uhlenbeck model (also called continuous-time correlated random walk, “CTCRW”), which has two parameters: ‘beta’ (mean reversion parameter) and ‘sigma’ (variance parameter), defined in Johnson et al. (2008). We define formulas for the SDE parameters to express covariate dependence, using the syntax from mgcv for smooth terms and random effects. Both parameters are specified as functions of the temperature covariate, using thin-plate regression splines,

```
# Model formulas for CTCRW parameters
formulas <- list(beta = ~ s(temp, k = 10, bs = "ts"),
                 sigma = ~ s(temp, k = 10, bs = "ts"))
```

We then create the SDE as an object, which encapsulates the data and model formulas,

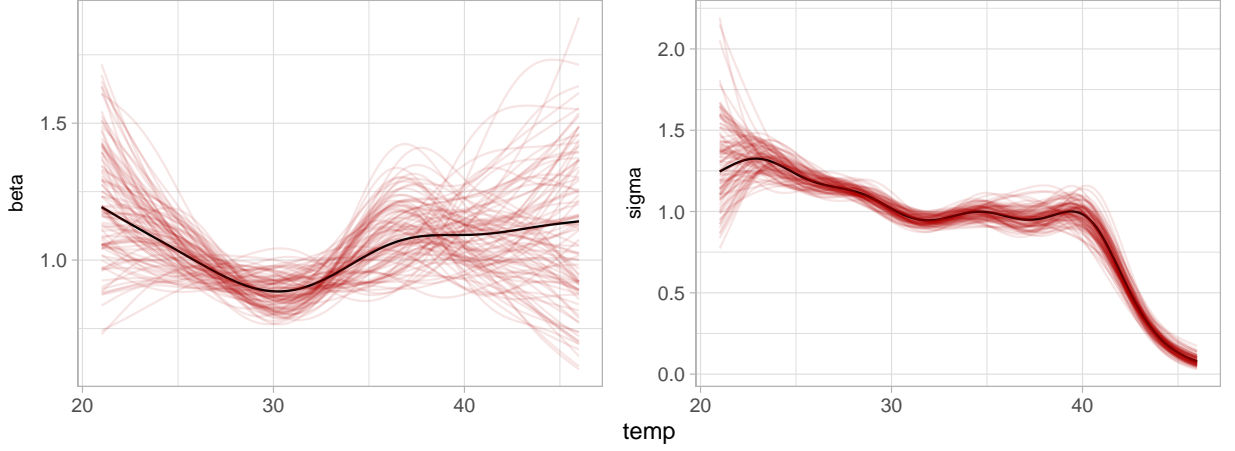
```
# Type of SDE model: continuous-time correlated random walk
type <- "CTCRW"

# Create SDE model object
my_sde <- SDE$new(formulas = formulas, data = track, type = type,
                  response = c("x", "y"))

# Fit model
my_sde$fit()
```

After model fitting, estimates of the SDE parameters, and posterior samples, can be plotted as functions of the covariates,

```
my_sde$plot_par("temp", n_post = 100)
```



Appendix C Simulation study

We ran simulations for two different model formulations, to investigate the performance of the inference method presented in Section 3 of the manuscript.

Scenario 1 We considered a Brownian motion with drift, where the parameters r_t (drift) and s_t (diffusion) were functions of a covariate x_{1t} . We generated the covariate as Brownian motion (with zero drift) over the time period of the simulations, and then scaled it to $[0, 1]$. For a choice of functions r_t and s_t (shown in Figure S2), we ran 50 simulations. For each, we simulated 10^5 data points at a fine time resolution ($\Delta = 0.01$) to make sure that the discretization error of simulation was negligible. We then downsampled the time series by keeping 2000 observations at random, to assess the performance of the method to recover the model parameters from data collected at irregular time intervals. We fitted the model to each downsampled data set, and derived estimates of r_t and s_t . Figure S2 shows the true r_t and s_t and the 50 estimates as functions of the covariate x_{1t} . The splines generally fitted the true functions well, although most of them did not capture the detailed oscillations in the drift parameter r_t over the lower end of the covariate range. This is because the smoothness of the true function varied over the covariate range (less smooth for low values, more smooth for high values), and the estimated smoothness can therefore be viewed as an average. This could be addressed with adaptive smoothing, i.e. by letting the degree of smoothness vary across values of the covariate (Wood, 2017, Section 5.3).

Scenario 2 In the second scenario, we assessed the performance of maximum likelihood estimation in the case where the diffusion process is not directly observed, and the Kalman

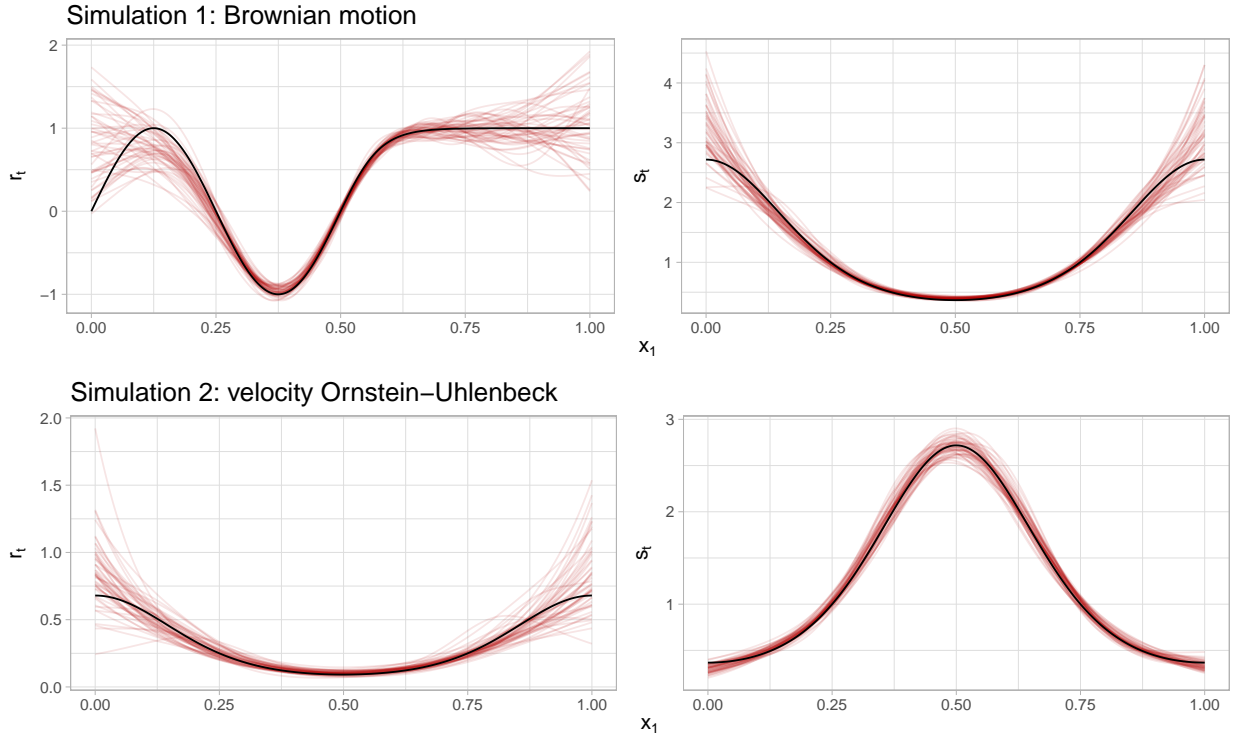


Figure S2: Results of simulation scenario 1 (top row) and scenario 2 (bottom row). The red lines are the 50 estimated drift parameters r_t and diffusion parameters s_t as functions of the covariate x_1 , and the black lines are the true functions.

filter needs to be implemented, as described in Section 2.2.1. We simulated 50 trajectories from the velocity OU model presented in Appendix A, following the same procedure as in the first scenario to obtain irregular observations. The parameters r_t and s_t used in the simulations were functions of one covariate, like in the previous scenario. We implemented the Kalman filter, to make inference about the parameters of the latent velocity process, based on the simulated observations. Figure S2 shows the results from the 50 simulations. The smoothness and general shape of both parameters r_t and s_t were recovered in all experiments.

Confidence interval coverage We ran another set of simulations to assess the coverage of Wald confidence intervals obtained using the joint precision matrix given by TMB (using `sdreport` as described in Appendix B.2). We simulated data from a varying-coefficient Brownian motion with drift, using the same drift and diffusion functions as in Scenario 1. Then, we fitted the model using TMB, and generated 1000 posterior samples for r_t and s_t on a grid over the covariate range. We derived pointwise 95% confidence intervals on that grid, and checked whether they included the true value. We repeated this experiment 1000 times, and derived the proportions of confidence intervals that included the true value. Average coverage over the covariate range was 95.3% for r_t and 96.7% for s_t , close to the expected 95%.

Appendix D Application to oil prices

This application involves the analysis of a time series of oil prices, inspired by García et al. (2017). We downloaded daily prices on WTI crude oil between 2 January 1986 and 30 March 2020 from the US Energy Information Administration website (eia.gov/dnav/pet/pet_pri_spt_s1_d.htm, accessed on 31 March 2020), and derived the log-returns as $R_i = \log(P_{i+1}/P_i)$ for day i , where P_i is the price of a barrel of crude oil. There were occasional missing values in this daily time series (easily accommodated in this continuous-time framework), resulting in a total of 8628 data points. We then fitted a varying-coefficient Brownian motion with drift to the log-returns R_i , where the drift and diffusion coefficients were specified as functions of the process value R_i . Model fitting took around 1 min on a 1.3GHz Intel i7 CPU.

Estimates of the drift parameter r_t and diffusion parameter s_t are shown as functions of the log-returns in Figure S3. Similarly to García et al. (2017), we found that the drift r_t was negative for positive log-returns, and positive for negative log-returns, i.e., the process

was attracted to zero. The diffusion parameter s_t increased with the absolute value of the log-returns, meaning that the process was more volatile when it took large (positive or negative) values. Based on a similar observation, García et al. (2017) suggested that s_t may be expressed as a quadratic function of the log-returns. Interestingly, our results indicate that this may be inappropriate, because the rate of increase of s_t decreases below -0.07 and above 0.07 .

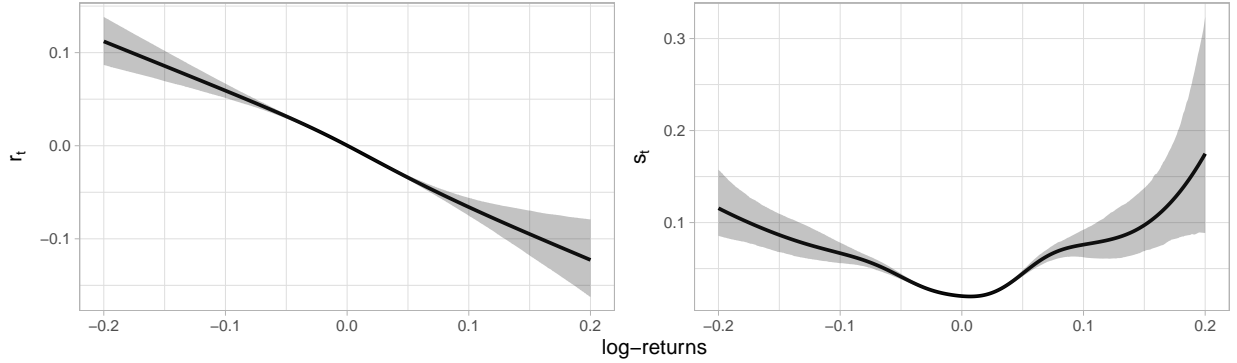


Figure S3: Results of crude oil price analysis, showing the drift parameter r_t and diffusion parameter s_t as functions of the log-returns. The black lines are the mean estimates, and the grey shaded areas are 95% confidence bands.

Appendix E Supplementary information for beaked whale analysis

E.1 Euler angles

Figure S4 shows an illustration of the three Euler angles derived from accelerometer data in the beaked whale analysis of Section 3.3: pitch, roll, and heading. They quantify the posture of the whale in the water.

E.2 Heavy-tailed model formulation

The three variables used in the beaked whale analysis of Section 3.3 of the main paper (pitch, roll, and heading) had heavy-tailed increments, which did not satisfy the assumption of normality made by Brownian motion. Here, we describe how we modified that model to accommodate the heavy tails.

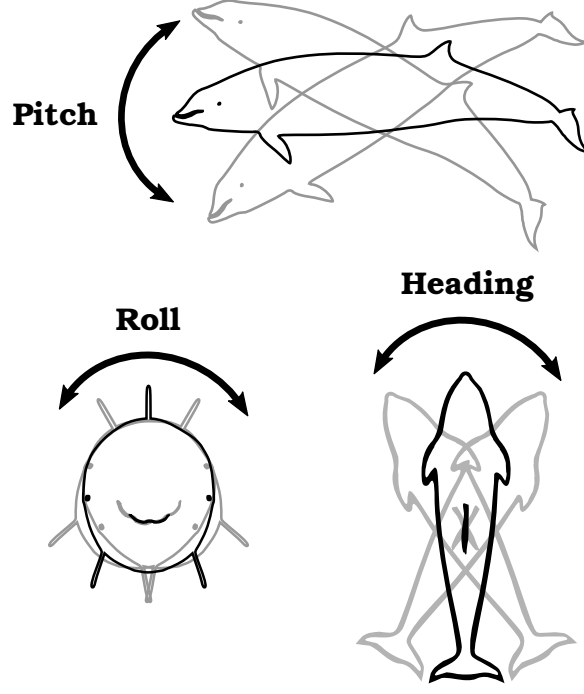


Figure S4: Illustration of Euler angles.

Formulation Let $D_i = Z_{t_{i+1}} - Z_{t_i}$ denote the increment in the process between two successive times of observation t_i and t_{i+1} . We write each process increment as

$$D_i = r_{t_i} \Delta_i + \tilde{s}_{t_i} \sqrt{\Delta_i} X_i$$

where

- $\Delta_i = t_{i+1} - t_i$ is the time interval;
- r_t is a time-varying location parameter;
- \tilde{s}_t is a time-varying scale parameter;
- for all i , X_i follows a Student's t distribution with $\nu > 2$ degrees of freedom.

Then, increments of the process follow a heavy-tailed generalized Student's t distribution, with mean $r_{t_i} \Delta_i$ and standard deviation $\tilde{s}_{t_i} \sqrt{\Delta_i} \sqrt{\nu/(\nu-2)}$. This is based on the standard assumption of Brownian motion that the increment mean scales linearly with the time interval, and the increment standard deviation scales linearly with the square root of the time interval. For ease of interpretation, in the paper we present results for the standard deviation parameter $s_t = \tilde{s}_t \sqrt{\nu/(\nu-2)}$ rather than for the scale parameter \tilde{s}_t .

Likelihood We consider n observations (z_1, \dots, z_n) from the process, collected at times $t_1 < \dots < t_n$. Under the assumption that increments are independent, we can write the full approximate likelihood as

$$L(\theta|z_1, \dots, z_n) = \prod_{i=2}^n [Z_{t_i} = z_i | Z_{t_{i-1}} = z_{i-1}, r_i, \tilde{s}_i],$$

where $r_i = r_{t_i}$ and $\tilde{s}_i = \tilde{s}_{t_i}$.

The transition density, i.e., the pdf of an increment of the process, is given by

$$[Z_{t_i} = z_i | Z_{t_{i-1}} = z_{i-1}, r_i, \tilde{s}_i] = f_X \left(\frac{z_{i+1} - z_i - r_i \Delta_i}{\tilde{s}_i \sqrt{\Delta_i}} \right) \times \frac{1}{\tilde{s}_i \sqrt{\Delta_i}},$$

where f_X is the pdf of a t distribution with ν degrees of freedom, and the term $1/(\tilde{s}_i \sqrt{\Delta_i})$ is the Jacobian of the transformation from X_i to the increment D_i .

Residuals We define the residuals of this model as

$$\epsilon_i = \frac{z_{i+1} - z_i - r_i \Delta_i}{\tilde{s}_i \sqrt{\Delta_i}}$$

using the notation from the previous sections. Under the assumptions of the model and the discretization, these residuals follow a t distribution with ν degrees of freedom.

E.3 ACF plots of residuals

Figure S5 shows autocorrelation function plots of the residuals for the three data variables in the beaked whale analysis (pitch, roll, and heading). Pitch and roll both display some negative autocorrelation over a few time lags (20-30 sec), which may be due to cycles in the motions of whales that were not captured by the model. The high positive autocorrelation in the residuals for heading suggest a strong tendency for whales to persist in the direction of rotation in the horizontal plane (i.e., either circling to the left or to the right).

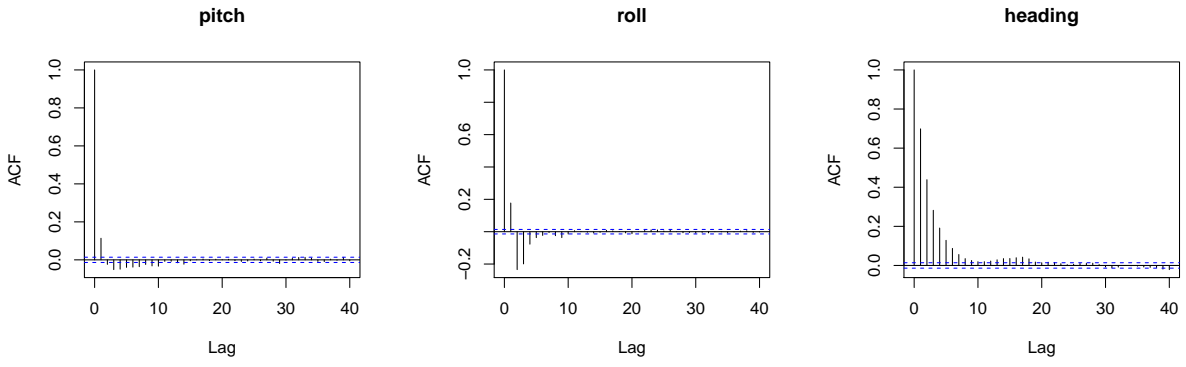


Figure S5: Autocorrelation function plots of residuals for beaked whale analysis. One lag unit corresponds to five seconds.